



Pentaerythritol as an excipient/solid-dispersion carrier for improved solubility and permeability of ursodeoxycholic acid.

Darshan R. Telange^a, Roshni P. Denge^a, Arun T. Patil^a, Milind J. Umekar^a, Sheeba Varghese Gupta^b, Vivek S. Dave^{c*}

^a Smt. Kishoritai Bhoyar College of Pharmacy, New Kamptee, Nagpur, Maharashtra, India

^b University of South Florida, College of Pharmacy, Tampa, FL, USA

^c St. John Fisher College, Wegmans School of Pharmacy, Rochester, NY, USA

Received: July 19, 2018; Accepted: September 13, 2018

Original Article

ABSTRACT

In this study, the feasibility of using pentaerythritol as a novel excipient/solid-dispersion carrier for enhancing the biopharmaceutical properties of ursodeoxycholic acid (UA) is explored. The solid dispersion formulations of UA were prepared using a solvent evaporation technique. The prepared formulations were evaluated for UA content to assess the efficiency of incorporating the UA into the formulation. The formulations were further characterized using photomicroscopy, scanning electron microscopy, particle size analysis, zeta potential analysis, infrared spectroscopy, thermal analysis, x-ray diffractometry, and performing solubility analysis. The performance of the selected formulation was evaluated by dissolution and permeability studies. A preliminary stability study was performed on the selected formulation. Solid dispersions of UA using pentaerythritol as a carrier were successfully prepared using UA providing efficiencies ranging from ~97 to 99%. The formation of dispersions was supported by instrumental analysis. Compared to pure UA, a 22-fold increase in aqueous solubility of UA was observed in the optimized formulation. The biopharmaceutical characteristics of UA, i.e., the rate and extent of dissolution and permeability, were found to be significantly increased in the optimized formulation compared with pure UA. The formulation was also functionally stable for six months when stored at controlled temperatures and humidity. This study shows that pentaerythritol can serve as a potential solid dispersion carrier for active pharmaceutical ingredients (API) and contribute to the enhancement of their biopharmaceutical properties.

KEY WORDS: Ursodeoxycholic acid, pentaerythritol, solid-dispersion, solubility, permeability, excipients

INTRODUCTION

Ursodeoxycholic acid (UA) is a naturally occurring secondary bile acid present in human bile ($\approx 4\%$) in the form of glycine or taurine conjugates (1-3). UA is a structural analog of chenodeoxycholic acid and these two bile acids have been employed for the treatment

of cholesterol gallstone diseases (4-6). UA has also been used for bile reflux gastritis and primary biliary cirrhosis (7, 8). Additionally, UA is reported to produce limited therapeutic effects such as immunomodulatory, anti-cancer, ulcerative colitis, and anti-inflammatory activities (9-12). Despite potential therapeutic benefits, oral and topical applications of UA are limited due to its poor aqueous solubility and low bioavailability (13, 14). Current literature reports a few approaches to enhance the solubility and bioavailability of UA

*Corresponding address: Vivek S. Dave, St. John Fisher College, Wegmans School of Pharmacy, Rochester, NY, 14534, Tel: +1 585 385 5297, Fax: +1 585 385 5295, E-mail: vdave@sjfc.edu

including β -cyclodextrin complexation, phospholipid complexation, and other nanotechnology-based approaches (15-18). While these approaches are promising, exploration of alternative, non-complex strategies/systems/approaches are warranted to enhance the bioavailability of UA and similar pharmacoactive compounds.

Solid dispersions are among the most effective approaches utilized for increasing solubility and permeability of poorly water-soluble drugs. A solid dispersion is essentially a dispersion of one or more drugs (commonly those from BCS class II and IV) in a polymeric inert carrier in solid state. Formation of successful solid dispersion largely depends on the nature of the solvent and the carrier. After selection of proper solvent and carrier/s, solid dispersion can be produced by melting, solvent-melting, solvent evaporation, or freezing based methods (19). Solid dispersions are known to improve the solubility, dissolution rate, and overall bioavailability of poorly water-soluble drugs through various mechanisms such as, reducing API particle size to sub-micron or smaller sizes, modification of crystalline API particles into high energy state amorphous particles providing larger surface areas, and enhancing the wettability of the drug particles in aqueous media due to the presence of highly water-soluble/hydrophilic inert carriers (20, 21).

Pentaerythritol is a white, crystalline organic solid compound with the formula $C_5H_{12}O_4$. It is a polyol with a neopentane backbone and one hydroxyl group in each of the four terminal carbons. It has a high aqueous solubility (56 mg/mL at 18°C). Due to the structural symmetry and low lattice energy of pentaerythritol, it can accommodate almost all classes of compounds, thus assisting in the formation of a solid dispersion. Pentaerythritol is among the least explored material, particularly with respect to its applications in drug delivery. Studies reporting pentaerythritol as a drug-delivery carrier are few and far between. The most relevant study appears to be by Chiou *et al.*, in 1969. The authors examined the feasibility of using pentaerythritol and pentaerythrityl tetraacetate, together with several grades of polyethylene glycols (PEGs) in preparing solid dispersions of griseofulvin, a low water-soluble, antifungal compound. The

study reported increased *in vitro* dissolution rates of griseofulvin in the pentaerythritol-based solid dispersions (22). No relevant studies exploring this bioavailability enhancing potential of pentaerythritol have been reported since.

Therefore, the main goal of the current study, was to explore the feasibility of using pentaerythritol as a relatively novel excipient/solid-dispersion carrier to enhance the biopharmaceutical characteristics of UA. Using ethanol-based solvent evaporation method solid dispersion formulations of UA with pentaerythritol (UA-SD) were prepared and evaluated. The prepared formulations were characterized for physicochemical properties using various analytical techniques including photomicroscopy, scanning electron microscopy, particle size analysis, zeta potential analysis, infrared spectroscopy, thermal analysis, x-ray diffractometry, and solubility analysis. The formulations were also evaluated for their UA solubilization and permeability properties. Finally, a preliminary, short-term study was conducted to assess the stability of the prepared formulations.

Materials and Methods

Materials

Ursodeoxycholic acid of high purity (> 98%) was obtained from Alkem Laboratories Ltd., Mumbai, India. Pentaerythritol was obtained from Sigma-Aldrich Corporation, St. Louis, MO, USA. Dichloromethane (DCM), ethanol, glacial acetic acid, soy lecithin, methanol, n-octanol sodium hydroxide and sodium taurocholate were acquired from Loba Chemical Pvt. Ltd., Mumbai, India. Other ingredients such as calcium chloride, glucose, magnesium sulfate, potassium chloride, potassium dihydrogen phosphate, sodium chloride and sodium bicarbonate were obtained from Merck Ltd. Mumbai, India, and were of analytical grade.

Preparation of pentaerythritol-based solid dispersions of ursodeoxycholic acid (UA-SD)

Several solid dispersion formulations of ursodeoxycholic acid (UA-SD) were prepared with

increasing stoichiometric ratios of pentaerythritol as a carrier, using an ethanol-based solvent evaporation method as reported previously (23). Briefly, accurately weighed pentaerythritol was transferred to a dry mortar. Separately, accurately weighed UA was dissolved in a sufficient quantity of ethanol in a clean beaker with magnetic stirring. This ethanolic solution of UA was then added to the mortar containing pentaerythritol. The dispersion was triturated to ensure uniform mixing and continued until complete evaporation of ethanol resulted in the formation of a solid mass. The residual solvent, if any, was removed by further subjecting this solid mass to vacuum drying at 40°C for 12 hours. The dried solid dispersion was sieved to obtain uniformly sized powders. The powder was then stored in light-resistant vials, flushed with nitrogen, at room temperature (25°C) until further use. The composition of the prepared formulations is shown in Table 1.

Table 1 Composition of the prepared Ursodeoxycholic acid-Pentaerythritol solid-dispersion formulations

FORMULATION	Ursodeoxycholic acid (mg)	Pentaerythritol (mg)
UA-SD1	100	100
UA-SD2	100	150
UA-SD3	100	200
UA-SD4	100	250
UA-SD5	100	300

Physicochemical characterization of UA-SD

Photomicroscopy and Scanning Electron Microscopy (SEM)

The particle morphology and surface characteristics of pure UA, pure pentaerythritol, and UA-SD were analyzed by photo-microscopy and scanning electron microscopy. For photo-microscopy, an aqueous dispersion of each sample (~2 mg/mL) was prepared and observed using a microscope (Model: DM 2500, Leica Microsystems, Germany). The images were obtained *via* the digital camera on the instrument.

For scanning electron microscopy, individual samples were uniformly spread on a double-sided carbon tape

affixed to an aluminum stub, which is then placed into the sample holder. The samples were then sputter-coated with a thin layer (400 Å) of gold/palladium. The coated samples were analyzed by scanning electron microscope (Supra[®] 55, Carl Zeiss NTS Ltd., Jena, Germany) equipped with Gemini[®] column, a graphical user interface (GUI), and an operating voltage acceleration range of 3-10 KV. The images were captured at various magnifications and analyzed using the proprietary software (SmartSEM[®] V05.06) associated with the instrument.

Particle size and zeta potential analysis

The mean particle size and spread of the prepared UA-SD formulations were evaluated using Photon Cross-Correlation Spectroscopy (PCCS) equipped with dynamic light scattering (DLS) technology (24). Briefly, ~5 mg of the UA-SD sample formulation was dispersed into 10 mL deionized water in a glass vial and stirred well. The vial was then mounted on the sample holder of the analyzer with a sensitivity range of 1 nm – 10 µm (Model: NANOPHOX Sympatec, GmbH, Clausthal-Zellerfeld, Germany). The particle size distribution of the samples was analyzed after optimizing the particle count rate by modifying the vial position.

The UA-SD formulations were also analyzed for any net surface charges by measuring the Dynamic Light Scattering (DLS) zeta potential on a nanoparticle analyzer (Model: NanoPlus[™]-2, Particulate system, Norcross, GA, USA) in the range of -200 to +200 mV. All measurements were performed at ambient temperature (25°C).

Thermal analysis

Thermal characterization of pure UA, pure pentaerythritol, the physical mixture (PM) of UA and pentaerythritol (1:2), and the prepared UA-SD formulation was carried out on a previously calibrated differential scanning calorimeter (Model: Q20, TA Instruments, Inc., New Castle, DE, USA) with a sensitivity of 1.0 µW, using the procedure reported by our group earlier (25). The samples were analyzed in a

moisture- and oxygen-free environment, assisted with a continuous purge of nitrogen (50 mL/min). The operating temperature range was set at 0°C to 400°C with ramp increments of 10°C/min. The resulting sample thermograms were analyzed with the associated software (TA Universal Analysis 2000, version 4.5A, build 4.5.0.5).

Fourier Transform Infrared Spectroscopy (FTIR)

FTIR spectral analysis of UA, pentaerythritol, PM, and UA-SD were performed to observe any drug-excipient interactions in the physical mixtures as well as solid dispersion formulations Fourier transform infrared spectrophotometer (Model: FTIR-8300, Shimadzu, Kyoto, Japan). The details of sample preparations, measurements, and data analysis were similar to those reported previously (24).

Powder X-ray Diffractometry (PXRD)

The crystalline nature of pure UA and pure pentaerythritol, as well as, any phase changes in their physical mixtures or in the prepared solid dispersion formulations, were assessed *via* x-ray diffractometry (Model: D8 ADVANCE, Bruker AXS, Inc., Madison, WI, USA). The employed methodology for testing individual samples was based on previous reports (24).

Estimation of UA in the prepared UA-SD

The incorporation efficiency of UA in the prepared SD formulations was estimated based on the procedure reported earlier by Choudhary et al. (26). Briefly, UA-SD (equivalent to ~100 mg UA) was accurately weighed, and dissolved in 100 mL phosphate buffer (0.05M, pH 6.8). The solution was then filtered using a membrane filter (0.45 μ m). The filtered solution, after appropriate dilutions, was measured for absorbance at $\lambda = 220$ nm on a UV-visible spectrophotometer (Model: V-630, JASCO International Co., Ltd., Tokyo, Japan) against a separately prepared solution of pentaerythritol to account for any interference.

Solubility analysis

The water-solubility of pure UA, as well as that

of UA present in the physical mixture, or the prepared UA-SD, were estimated using the method previously described by Al-Hamidi et al. (27). Briefly, a suspension of individual samples was prepared by adding an excess amount of pure UA, PM, or UA-SD formulation to a vial (glass) containing 10 mL distilled water. The suspension was agitated on a rotary shaker (Model: RS-24 BL, REMI Laboratory Instruments, Remi House, Mumbai, India) at 37°C for a period of 24 hours. The suspension was then filtered *via* membrane filter (0.45 μ m). The aliquots of the collected filtrate, after appropriate dilutions were analyzed for UA concentration at $\lambda = 228$ nm on a UV-visible spectrophotometer (Model: V-630, JASCO International Co., Ltd., Tokyo, Japan).

Functional characterization of UA-SD

***In vitro* dissolution studies**

The dissolution properties of pure UA and UA-SD were evaluated with the USP method II (paddle method) on a dissolution tester (Model: TDT-08LX, Electrolab India Pvt. Ltd., Mumbai, India). The samples of pure UA (100 mg) or UA-SD formulation (equivalent to ~100 mg UA) was dispersed onto continuously stirred (100 RPM) dissolution media (Phosphate buffer, 0.05 M, pH 6.8), maintained at $37 \pm 0.5^\circ\text{C}$. For analysis, aliquots of samples were withdrawn at predetermined intervals and filtered (0.45 μ m). The sink conditions in the dissolution vessels were maintained by replenishing with fresh medium in quantities equal to those of the withdrawn samples. The filtered analyte, after suitable dilutions, was assayed for UA absorbance at $\lambda = 204$ nm on a UV-visible spectrophotometer (Model: V-630, JASCO International Co., Ltd., Tokyo, Japan). Temporally obtained absorbance values were converted into cumulative dissolution profiles (%) for the purpose of reporting.

Comparison of UA dissolution in fasted vs fed state

The food effect on the dissolution properties of UA-SD was tested using Fasted-State Simulated Intestinal Fluid (FaSSIF) and Fed-State Simulated Intestinal Fluid (FeSSIF) as dissolution media. The blank FaSSIF

and FeSSIF media were prepared by following the procedures reported earlier (28). USP type II (paddle method) dissolution apparatus (Model: TDT- 08LX Electrolab India Pvt. Ltd., Mumbai, India) was used to perform dissolution studies in FaSSIF (500 mL) or FeSSIF (1000 mL) media continuously stirred at 50 RPM, and maintained at $37 \pm 0.5^\circ\text{C}$. Aliquots of samples (10 mL) were withdrawn at 10 min intervals, membrane-filtered ($0.45 \mu\text{m}$), and assayed for UA absorbance at $\lambda = 273 \text{ nm}$ (for FaSSIF) and $\lambda = 306.6$ (for FeSSIF) on a UV-visible spectrophotometer.

Ex vivo permeability

The permeability characteristics of pure UA and UA-SD were comparatively analyzed by the *everted rat intestine method* reported earlier by Dixit et al. (29). The details regarding instrument design, tissue isolation, and sample collection used in this study are previously reported by our group (23, 30, 31). The use of experimental animals in this study was approved by the *Institutional Animal Ethics Committee* (IAEC), and the experimental protocol followed the ethical guidelines of the *Committee for the Purpose of Control and Supervision of Experiments on Animals* (CPCSEA). The analyte samples collected at regular time intervals were spectrophotometrically analyzed at $\lambda = 240 \text{ nm}$ to estimate the permeability of UA across a biological barrier.

Preliminary stability analysis of UA-SD

The functional stability of the prepared UA-SD formulations was assessed by conducting a preliminary stability analysis of the samples for six months at temperature and humidity conditions of $25 \pm 2^\circ\text{C}$ and $60 \pm 5\% \text{ RH}$, respectively. The SD formulations were packed in screw-capped, amber-colored glass vials, and the vials were placed in a temperature- and humidity-controlled environmental chamber (Model: TS00002009, Mumbai, India) for six months. At the end of assigned storage duration, the samples were retrieved and assessed for their functionality (dissolution and permeability of UA).

Statistical analysis

All of the results are shown as mean \pm standard

deviations. The statistical differences between the prepared SD formulations was carried out by performing a one-way Analysis of Variance (ANOVA) followed by Dunnett or Student's t-test. For group comparisons, a P value of ≤ 0.05 , were assumed as statistically significant.

RESULTS AND DISCUSSION

Physicochemical characterization of UA-SD

Photomicroscopy and Scanning Electron Microscopy (SEM)

Figure 1A and 1B show the photo-microscopic and scanning electron microscopic characterization of pure UA (a1 and b1), pure pentaerythritol (a2 and b2), and the prepared UA-SD (a3 and b3), respectively. Pure UA appeared as small, relatively transparent, regular-shaped, crystalline particles with sharp edges in optical microscopy. The SEM revealed a smooth surface morphology of these crystals. Pure pentaerythritol appeared as small, transparent, heterogeneous and somewhat smooth-edged crystals. The surface morphology of pentaerythritol as revealed by SEM showed the heterogeneous distribution with a relatively non-smooth surface. The UA-SD appeared in the form of clusters with undefinable shape or form. The SEM images of the UA-SD showed fused particles with characteristics of UA and pentaerythritol.

Particle size and zeta potential analysis

Figure 2A and 2B shows the particle size distribution and the measured zeta potential of the prepared UA-SD particles, respectively. The mean particle size of UA-SD was observed to be $\sim 780 \text{ nm}$. Moreover, these particles exhibited a relatively lower polydispersity index of 0.34 ± 0.07 , indicating a narrow range of size distribution. Earlier reports have suggested that sub-micron particles are absorbed by the intestinal epithelium *via* cellular uptake, and can be suitable for oral administration (32). In addition to the desired size and size-spread of such particles, measuring the surface charge on the particles (zeta potential, ζ) can provide some insights into the possible fate of sub-micron particles after oral administration (33). The

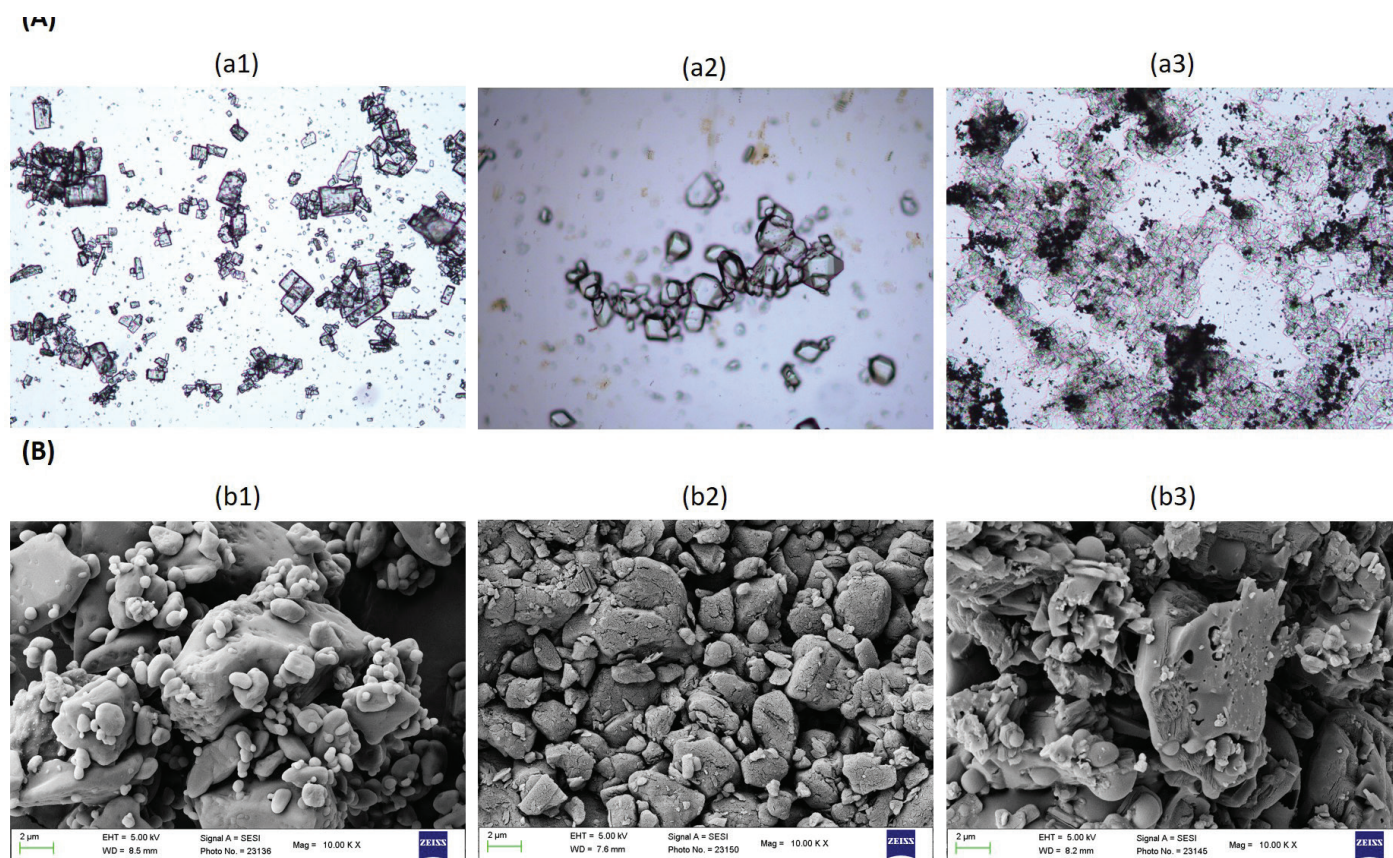


Figure 1 A) The photomicroscopy images of (a1) pure ursodeoxycholic acid (UA), (a2) pure pentaerythritol, and (a3) the prepared solid dispersion of UA with pentaerythritol. B) The scanning electron micrographs of (b1) pure ursodeoxycholic acid (UA), (b2) pure pentaerythritol, and (b3) the prepared solid dispersion of UA with pentaerythritol.

zeta potential values in the range of -30 mV to $+30$ mV are considered to be acceptable for the physical stability of multiparticulate systems. The tested UA-SD samples exhibited the zeta potential values of ~ 15 mV and was considered to be within an acceptable range.

Thermal analysis (DSC)

The thermal properties of pharmaceutical materials (active pharmaceutical ingredients and excipients) are unique, and close proximity of different materials in a formulation may influence these properties. Any interaction between formulation components resulting in a modification of thermal properties may be exhibited as appearance, disappearance or shifting of specific thermal peaks in response to changes in temperature. Thermal analysis of individual components, and the formulation as a whole, is also important to ensure compatibility between the components and often

support the formation of a desired entity.

Thermograms of pure UA, pure pentaerythritol, PM, and UA-SD are presented in Figure 3 (A-D), respectively. Pure UA (Figure 3A) exhibited a well-defined endothermic peak at $\sim 206^{\circ}\text{C}$ and can be assumed to be the melting peak of UA (34). Pentaerythritol thermogram showed two dissimilar endothermic peaks (Figure 3B). First broad peak appeared around $\sim 196^{\circ}\text{C}$ and is possibly due to the phase transition of pentaerythritol from its usual tetragonal form (crystal structure II) to cubic lattice structure (crystal structure I). These changes were also supported by the reported entropy of transition of ~ 23 Cal/degree/mole. Second small diffused endothermic peak was exhibited at $\sim 281.5^{\circ}\text{C}$, indicating the melting of pentaerythritol (22, 35). Figure 3C displays the thermal characteristics of the physical mixture and exhibited a two endothermic peaks at around $\sim 193^{\circ}\text{C}$ and $\sim 257^{\circ}\text{C}$, respectively. The first endothermic peak is

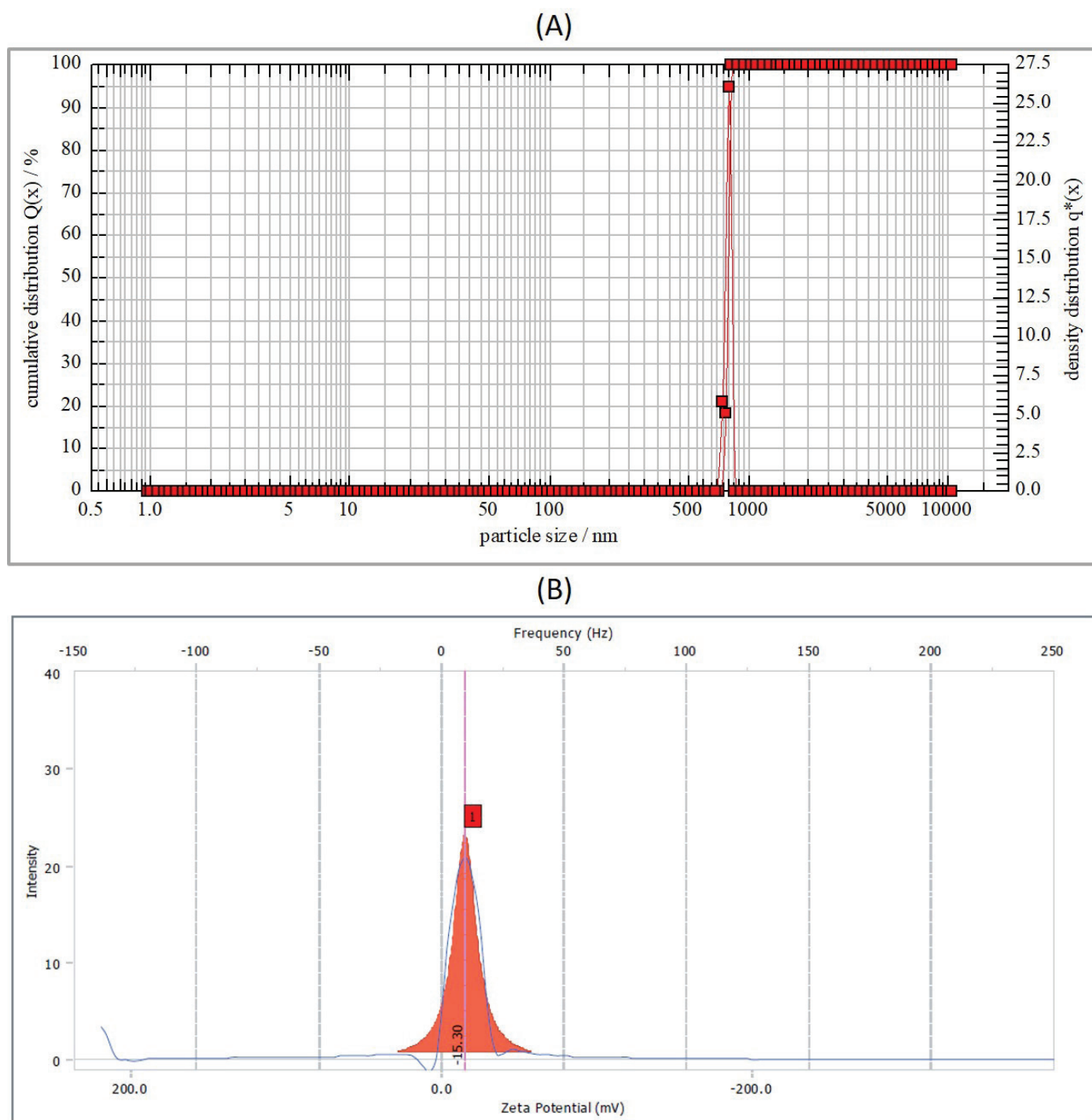


Figure 2 Particle size distribution (A) and zeta potential (B) of the prepared solid dispersion of UA with pentaerythritol.

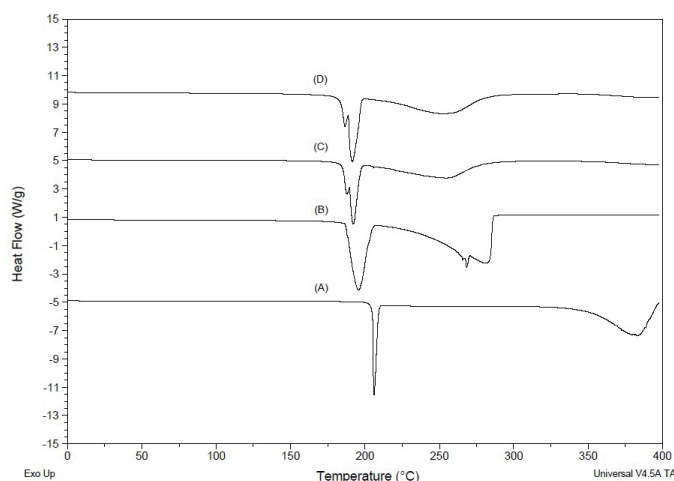


Figure 3 DSC thermograms of (A) pure ursodeoxycholic acid, (B) pure pentaerythritol, (C) the physical mixture (1:2) of ursodeoxycholic acid and pentaerythritol, and (D) the prepared solid dispersion of UA with pentaerythritol.

related to pure ursodeoxycholic acid, whereas, second endothermic peak corresponds to pentaerythritol. The appearance of these two peaks in the thermogram indicated an interaction between the components. However, the melting point and intensity of both peaks were observed to be lower compared to pure UA and pure pentaerythritol. This could be attributed to a possible interaction between the components to increasing temperature, as well as the possible formation of a new entity with lower melting point. The lower intensities of peaks may be attributed to the relative quantities of components and sample size. The UA-SD thermogram (Figure 3D) was somewhat similar to that of the PM and revealed two dissimilar endothermic peaks. First endothermic peak appeared at $\sim 192^{\circ}\text{C}$, whereas, the second diffused peak observed at $\sim 250^{\circ}\text{C}$. Compared to original peaks of pure UA and pure pentaerythritol, the peaks in UA-SD thermogram were observed to be dramatically different. These changes indicated an interaction between the components of UA-SD and possible formation of a solid dispersion. Furthermore, the phase transition of pentaerythritol may reduce the crystallinity of UA by accommodating it into the crystal lattice lead to formation of UA-SD solid-dispersion with amorphous characteristics (22, 34).

Fourier Transform Infrared Spectroscopy (FTIR)

The comparative infrared spectra of pure UA, pure pentaerythritol, PM, and UA-SD are shown in **Figure 4** (A-D), respectively. As shown in Figure 4A, pure UA spectrum exhibited four unique absorption signals; the -OH stretching signals at 3500.95 cm^{-1} and 3231.87 cm^{-1} , and C=O stretching signals at 1716.72 cm^{-1} and 1694.54 cm^{-1} . These observations are in agreement with those reported earlier (34). Pentaerythritol spectrum (Figure 4B) exhibited characteristic and previously reported absorption peaks at 3325.42 cm^{-1} (-OH stretching), 2942.53 cm^{-1} (asymmetric C-H stretching), 1217.14 cm^{-1} and 1129.37 cm^{-1} (C-C stretching), 1041.61 cm^{-1} and 1013.64 cm^{-1} (C=O stretching) (36). The FTIR spectrum of the physical mixture (Figure 4C) exhibited absorption signals at 3497.09 cm^{-1} , 3317.71 cm^{-1} , 2942.53 cm^{-1} , 1716.72 cm^{-1} , 1129.37 cm^{-1} , 1041.61 cm^{-1} , 1013.64 cm^{-1} . These peaks corresponded to the specific components of the mixture i.e., UA and pentaerythritol, albeit with altered intensities and shifts, as expected. The infrared absorption spectrum of the prepared UA-SD solid-dispersion revealed peaks that were significantly altered compared to those observed with the individual components (Figure 4D). For example, the peak at 3231.87 cm^{-1} (pure UA) shifted to 3297.45 cm^{-1} in UA-SD formulation, indicating the involvement of weak intermolecular forces such as hydrogen bonding and ion-dipole forces between the components. Other peaks at 3325.42 cm^{-1} , 1217.14 cm^{-1} , 1129.37 cm^{-1} , 1041.61 cm^{-1} and 1013.64 cm^{-1} appeared similar to that of pentaerythritol spectrum, indicating that these functional groups did not contribute to the interaction mechanism. These results support the formation of molecular adducts of UA and pentaerythritol in the prepared UA-SD.

Powder X-ray Diffractometry (PXRD)

PXRD is typically employed as a supportive technique to understand the crystalline behavior of the components of a formulation. Any changes in the crystal properties of an API as a result of formulation into a solid dispersion with a carrier can be identified by PXRD analysis. For the current study, the x-ray diffraction characteristics of pure UA, (Figure 5A) The diffraction

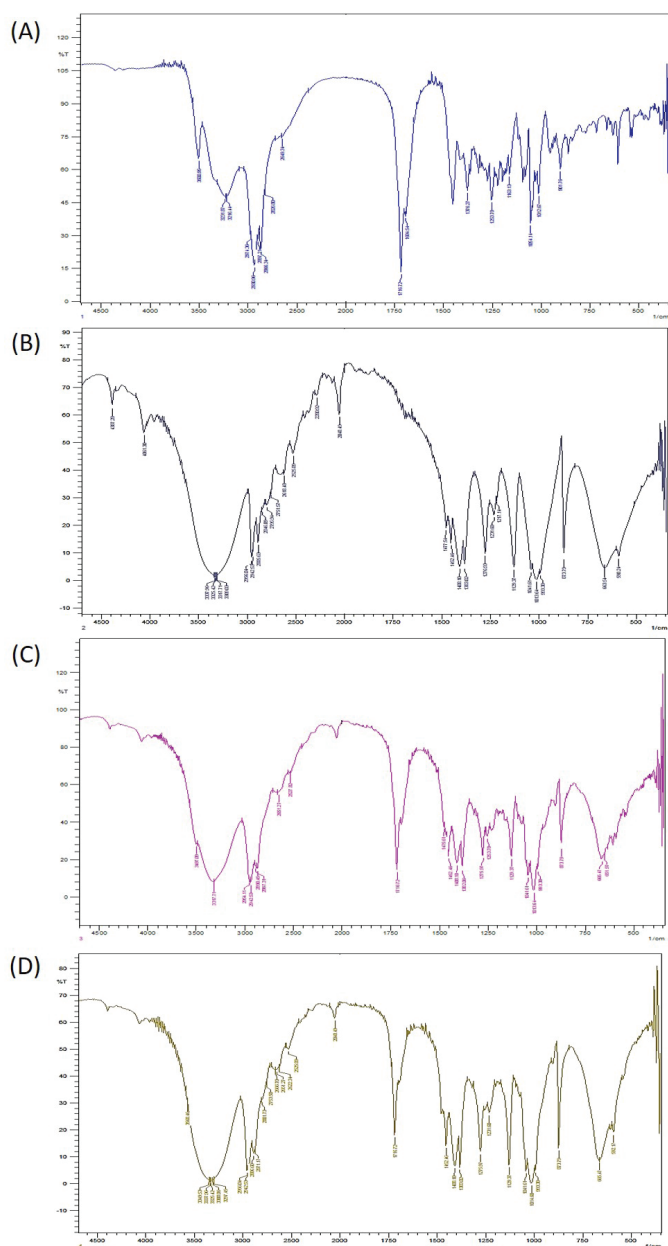


Figure 4 FTIR spectra of (A) pure ursodeoxycholic acid, (B) pure pentaerythritol, (C) the physical mixture (1:2) of ursodeoxycholic acid and pentaerythritol, and (D) the prepared solid dispersion of UA with pentaerythritol.

pentaerythritol, PM, and UA-SD are shown in Figure 5 (A-D), respectively. revealed several sharp, crystalline peaks between 7° and 26° . This characteristic diffractive pattern of UA, indicative of its crystalline nature, was observed to be similar to that reported earlier (18).

pattern of pentaerythritol (Figure 5B) exhibited one prominent peak at 20° , and other peaks of relatively lower intensities at 18° , 29° , and 36° . The defining peak of pentaerythritol (at 20°) was found to be of high intensity ($\sim 55,000$ counts), and several orders of magnitude higher compared to those of pure UA. This diffractogram was characteristic of the crystal lattice of pentaerythritol and has been previously reported (22). Figure 5C shows the diffractogram of the physical mixture of UA and pentaerythritol. This diffractogram revealed mainly the characteristic sharp peaks associated with pentaerythritol, albeit with lower intensities. The diffraction peaks of UA in this physical mixture appeared to have been suppressed, likely due to the dominance of pentaerythritol. The diffraction patterns of UA-SD (Figure 5D) predominantly showed the characteristic peaks of pentaerythritol with a few, ill-defined, broad, low intensity, peaks that may be related to the presence of UA in partially amorphized form within the solid dispersion. For the reason explained in the sections above, i.e., the low lattice energy of pentaerythritol allowing molecular dispersion of UA to occur freely, possibly resulted in the disappearance of the crystalline peaks of UA (20, 22).

Estimation of UA in the prepared UA-SD

The results of the estimated UA incorporation in

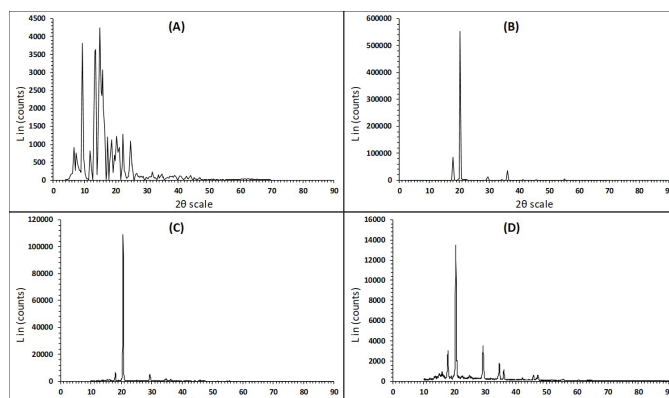


Figure 5 The x-ray diffractograms of (A) pure ursodeoxycholic acid, (B) pure pentaerythritol, (C) the physical mixture (1:2) of ursodeoxycholic acid and pentaerythritol, and (D) the prepared solid dispersion of UA with pentaerythritol.

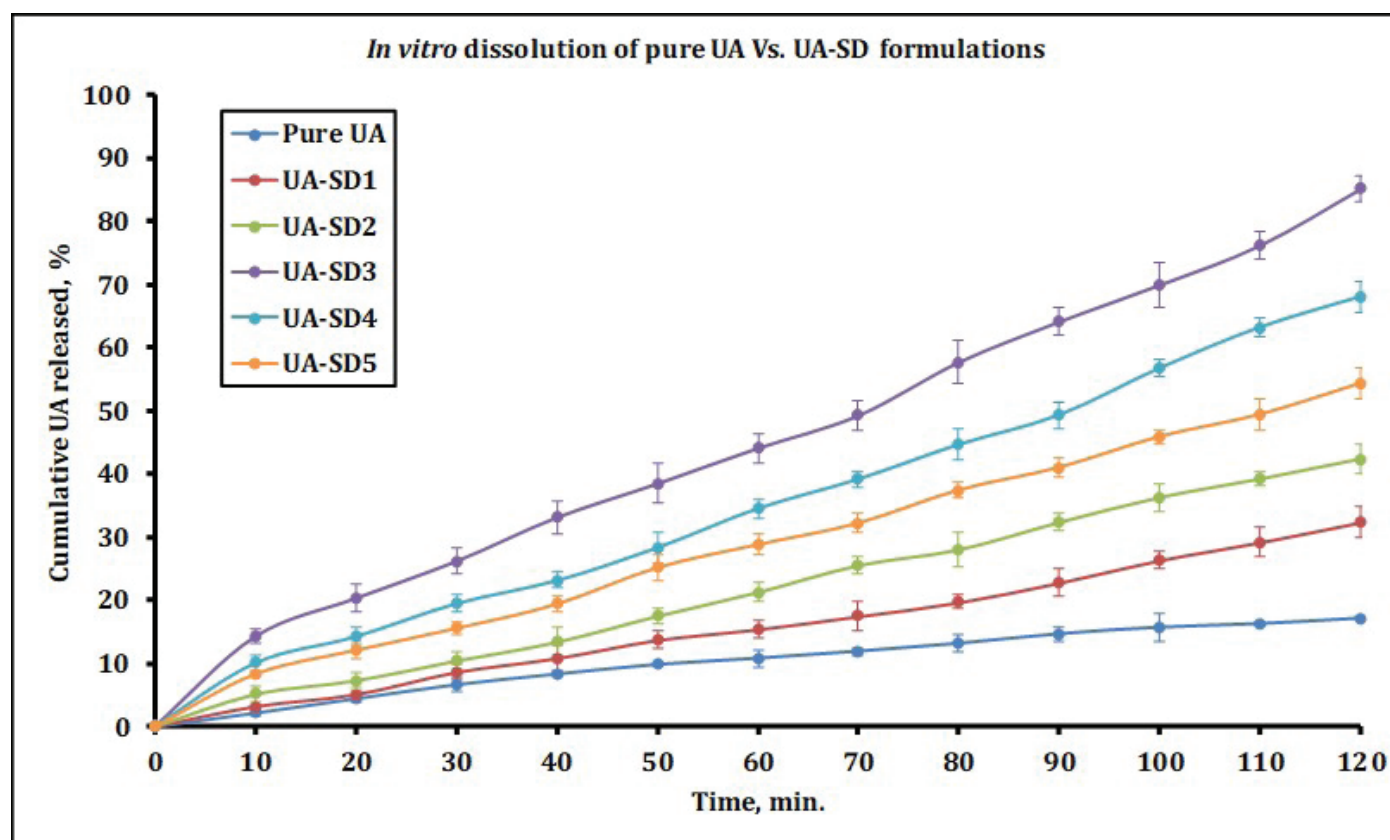


Figure 6 Comparative dissolution profiles of pure ursodeoxycholic acid, and ursodeoxycholic acid in the prepared UA-SD formulations in phosphate buffer (pH-6.8). Values are mean \pm Std. Dev. (n = 3).

the prepared UA-SD trial formulations are shown in Table 2. All of the prepared UA-SD trial formulations exhibited a high incorporation efficiency of UA with the UA content ranging from 97 to 99 %, w/w. The UA incorporation in formulation UA-SD3 was observed to be 99.26 ± 1.18 (% w/w), and was thus selected for further evaluation. Overall, the high incorporation efficiency of UA in the prepared solid dispersion formulations demonstrated the feasibility and validity of the method of preparation.

Solubility analysis

The results obtained from the aqueous solubility analysis of pure UA, UA in the physical mixtures with various ratios of pentaerythritol, as well as that of UA in the prepared trial UA-SD formulations are shown in Table 3. The estimated aqueous solubility of pure UA was 0.54 ± 0.04 $\mu\text{g}/\text{mL}$ and can be categorized as a BCS class II entity (18). The aqueous solubility of UA in

the physical mixtures increased with stoichiometrically increasing ratios of pentaerythritol, possibly due to close proximity of UA to the highly water-soluble pentaerythritol molecules in the mixture. The solubility of UA in the UA-SD formulations were observed to be significantly (several orders of magnitude) greater compared to that observed with pure UA or UA in the physical mixtures. The formulation UA-SD3 demonstrated the highest aqueous solubility of UA

Table 2 Ursodeoxycholic acid (UA) incorporation efficiency in the prepared formulations

FORMULATION	ESTIMATED UA CONTENT (% w/w of theoretical)
UA-SD1	97.10 ± 1.12
UA-SD2	98.09 ± 1.07
UA-SD3	99.26 ± 1.18
UA-SD4	98.70 ± 0.58
UA-SD5	97.37 ± 1.21

Values are mean \pm Std. Dev (n = 3)

Table 3 Aqueous solubility of pure UA, UA in the physical mixtures (PM), and UA in the prepared solid-dispersion formulations

FORMULATION	AQUEOUS SOLUBILITY ($\mu\text{g/mL}$)
Pure ursodeoxycholic acid	0.54 ± 0.04
PM-1	0.57 ± 0.06
PM-2	0.59 ± 0.02
PM-3	0.62 ± 0.02
PM-4	0.63 ± 0.05
PM-5	0.65 ± 0.03
UA-SD1	4.31 ± 0.05
UA-SD2	6.31 ± 0.05
UA-SD3	12.10 ± 0.08
UA-SD4	11.04 ± 0.05
UA-SD5	9.11 ± 0.04

Values are mean \pm Std. Dev ($n = 3$)

i.e., $12.10 \pm 0.08 \mu\text{g/mL}$. This was over 22-fold higher water-solubility compared to that of pure UA. The interactions of UA with pentaerythritol at a molecular level, as well as possible partial amorphization of UA in the prepared formulations are thought to result in observed enhancement of aqueous solubility of UA in these formulations (37, 38).

Functional characterization of UA-SD

In vitro dissolution studies

Comparative dissolution profiles of pure UA and UA-SD formulations in phosphate buffer (pH-6.8) are shown in Figure 6. The dissolution behavior of the physical mixtures of UA and pentaerythritol are not reported; preliminary dissolution studies on the physical mixture showed dissolution profiles overlapping that of pure UA i.e., no significant differences were observed between the dissolution behavior of pure UA and those of UA in the mixtures. Pure UA exhibited a lower rate and extent of solubilization with only $\sim 17\%$ UA solubilized over a period of two hours. These observations are expected, owing to the low aqueous solubility of UA, and consistent with earlier reports (18). With various UA-SD formulations, the rate and extent of UA solubilization was observed to be significantly enhanced compared to that of pure UA. In general, the dissolution of UA appeared to follow a near-linear

path in these formulations. Moreover, the dissolution profiles appeared to directly correlate with the aqueous solubility of UA in these formulations. For example, UA-SD3 which exhibited the highest solubility of UA also demonstrated highest rate and extent of UA dissolution. At the end of two-hour evaluation period, over 85% of UA was observed to be solubilized in this formulation. The observed enhanced dissolution of UA in these formulations can be likely due to the formation of high energy solid-state formulation by solvent evaporation method, i.e. partial amorphization of drug dispersed in a carrier (34). Carrier with low lattice energy compounds easily accommodates highly ordered crystallized compounds for the formation of molecular dispersion *via* reducing particle size with high surface area for improved dissolution rate (22). Additionally, highly water-soluble carriers such as polymers are also known to reduce nucleation, crystal growth, and re-precipitation of amorphous drug in a supersaturated solution, thus improving dissolution (39).

Comparison of UA dissolution in fasted vs fed state

Figure 7 shows the food-effects on the solubilization behavior of pure UA, and UA in the selected UA-SD3 formulation as tested in fasted (FaSSIF) and fed (FeSSIF) conditions. In fasted conditions, pure UA exhibited a lower rate and extent of dissolution. At the end of the 2-hour testing period, only $\sim 17\%$ UA was solubilized. In fed conditions the rate and extent of UA dissolution appeared to be moderately but significantly greater, i.e., $\sim 26\%$ UA was found to be solubilized at the end of testing period. Positive food effects on the solubilization of drugs with low water-solubility is well-known (28, 40). The rate and extent of UA dissolution from the UA-SD3 in fasted conditions, was found to be greater compared to that observed with pure UA in both fasted and fed conditions. At the end of the two-hour evaluation, $\sim 39\%$ UA appeared to be released. These results are not surprising as they correlate well with both, the solubility analysis and the *in-vitro* dissolution results. In fed conditions, UA-SD3 exhibited a dramatic and a greatly increased rate and extent of UA dissolution, i.e. $\sim 89\%$ UA was found to be solubilized at the end of 2 hours. The observed

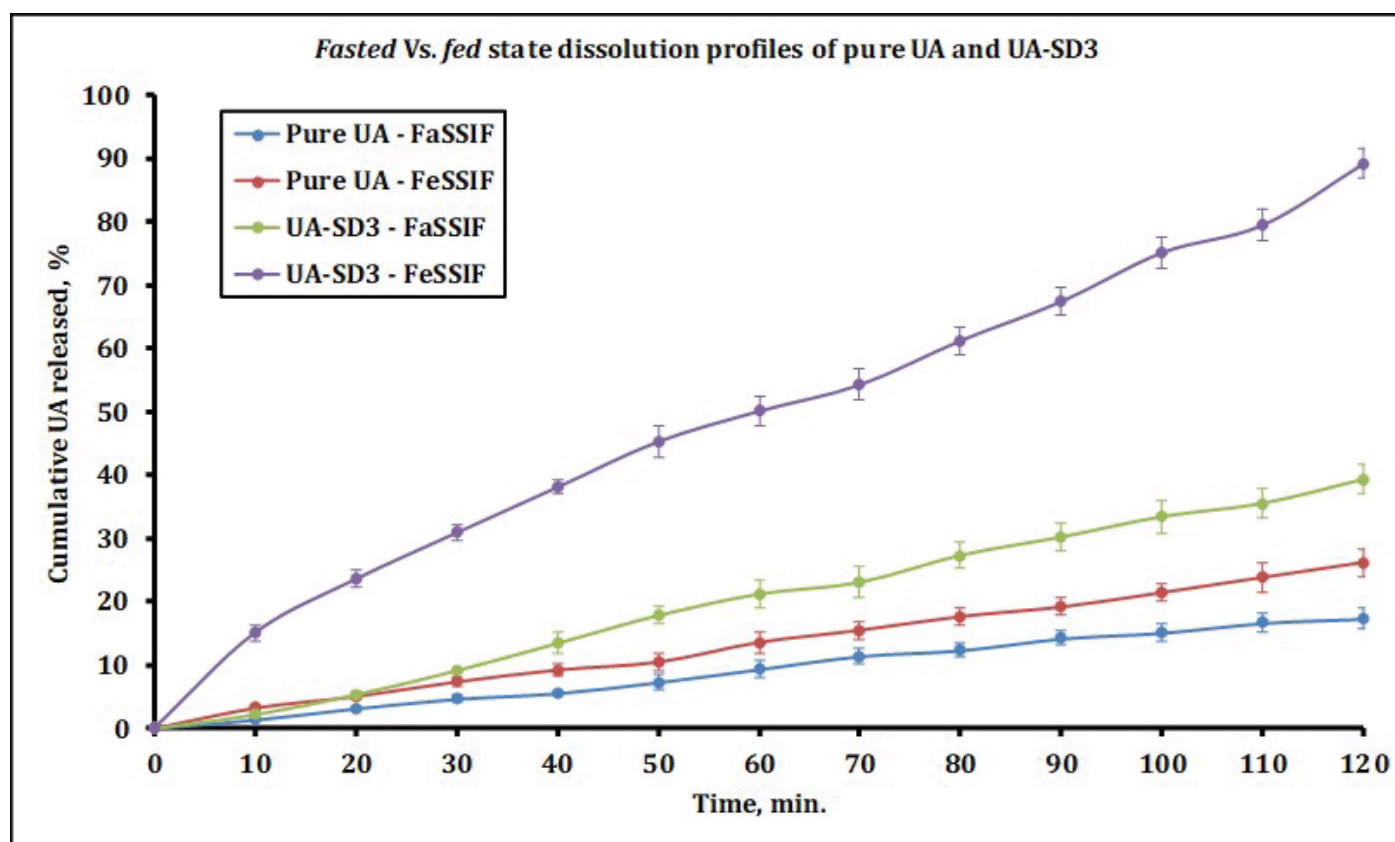


Figure 7 Comparative dissolution behavior of pure ursodeoxycholic acid, and ursodeoxycholic acid in the selected UA-SD3 formulation as tested in fasted (FaSSIF) and fed (FeSSIF) conditions. Values are mean \pm Std. Dev. (n = 3).

enhancement in the rate and extent of UA solubilization could be attributed to the synergistic effects of the positive food effects and partial amorphization of UA in the prepared solid dispersion on UA solubility.

Ex vivo permeability

The comparative permeabilities of pure UA and UA in the prepared UA-SD formulations across a biological membrane barrier, as tested using the *everted rat intestine* method, are shown in Figure 8. Pure UA showed the lowest permeability (rate and extent) compared to all the tested formulations. Only ~18% UA was observed to be perfused across the rat intestinal membrane at the end of 2-hour testing period. The UA-SD formulations, however, exhibited a statistically significant and greater rate and extent of UA permeability. The permeability profiles of the individual formulations mimicked their dissolution behavior, as well as correlated with the

aqueous solubility of UA in these formulations. The formulation UA-SD3, which showed highest aqueous solubility and dissolution rate of UA, also demonstrated the highest rate and extent of permeability. At the end of the evaluation period, over 87% UA appeared to have permeated across the biological membrane. The same reasoning discussed above can be attributed to the observed enhancement of UA permeability in these formulations.

Preliminary stability analysis of UA-SD

The results obtained from the 6-month, a preliminary stability assessment of the selected UA-SD preparation are shown in Figure 9. Figure 9A compares the solubilization profiles of UA-SD3 initial formulation (day 0), and that stored under controlled conditions of temperature and humidity for six months (day 180). As observed, the dissolution behavior of both samples overlapped, i.e. the differences in the solubilization

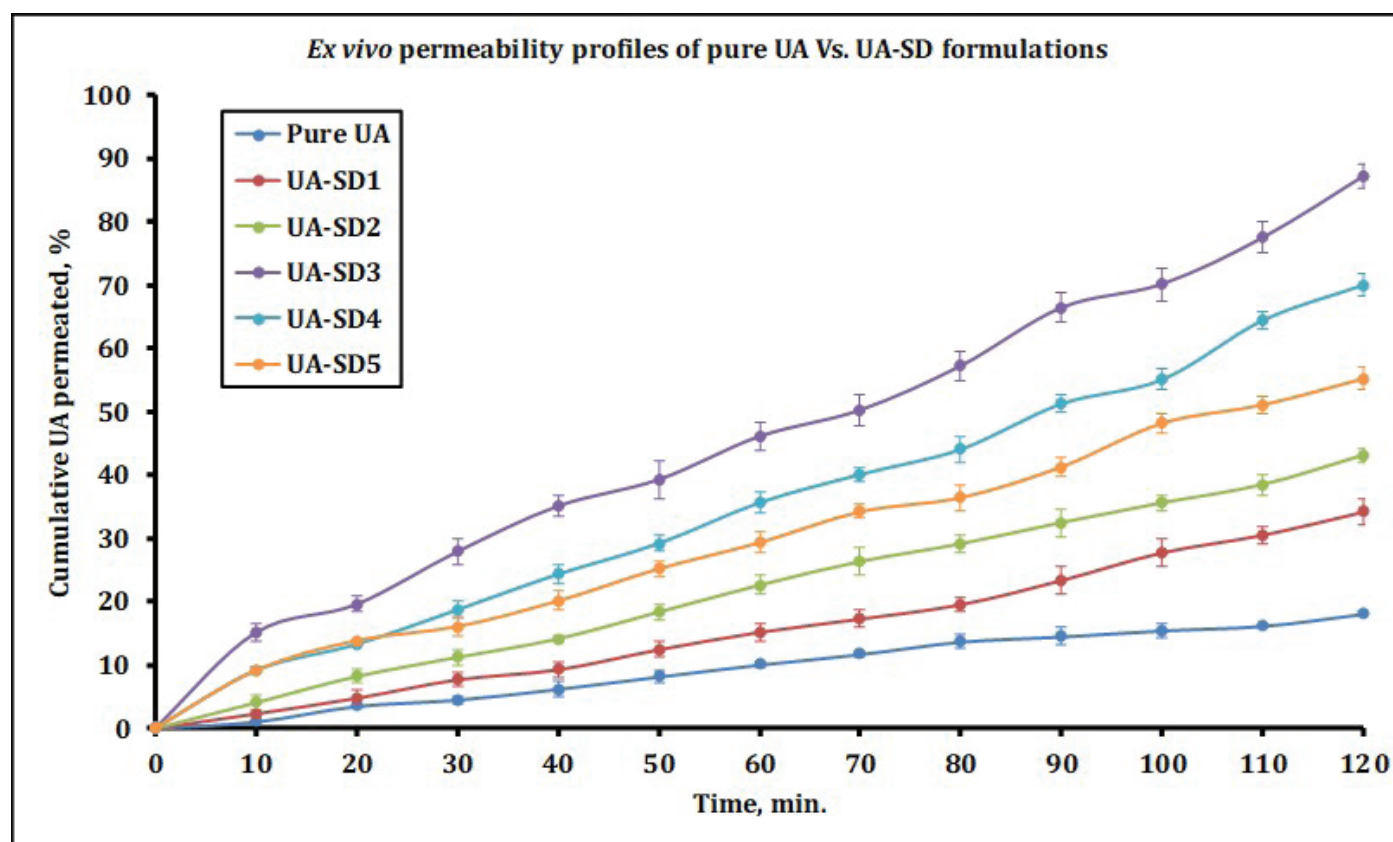


Figure 8 Comparative permeabilities of pure ursodeoxycholic acid, and ursodeoxycholic acid, in the prepared UA-SD formulations across a biological membrane barrier, as tested using the everted rat intestine method. Values are mean \pm Std. Dev. ($n = 3$).

profiles of UA from these formulations were not found to be statistically significant as a function of storage. Similarly, a comparison of the permeability profiles of UA-SD3 initial formulation (day 0) with that stored for six months (day 180) showed a nearly identical rate and extent of UA permeability across the biological barrier upon storage (Figure 9B). The storage conditions did not appear to have a significant effect on the solubilization or permeation characteristics of UA. UA was likely maintained in a partially amorphous state within the dispersion. Of course, further detailed stability analysis is warranted to substantiate this claim.

CONCLUSIONS

In the current study, the authors explored the feasibility of utilizing pentaerythritol as a non-traditional excipient/solid-dispersion carrier to enhance the biopharmaceutical characteristics of ursodeoxycholic acid. Solid-dispersion formulations of UA using

various ratios of pentaerythritol were prepared using an easy to perform, solvent-evaporation technique. The prepared formulations were characterized for physical-chemical and functional attributes and compared with pure UA. The physical-chemical characterization revealed that the interactions between UA and pentaerythritol are likely mediated *via* intermolecular forces such as hydrogen bonding and/or ion-dipole interactions. The prepared formulations significantly improved the water-solubility of UA. The functional characterization of the formulations showed a greater rate and extent of UA solubilization and pervasion across biological membrane. The preliminary stability assessment indicated that the prepared formulations are stable. These encouraging results warrant further investigation of pentaerythritol as a novel excipient/drug-delivery carrier.

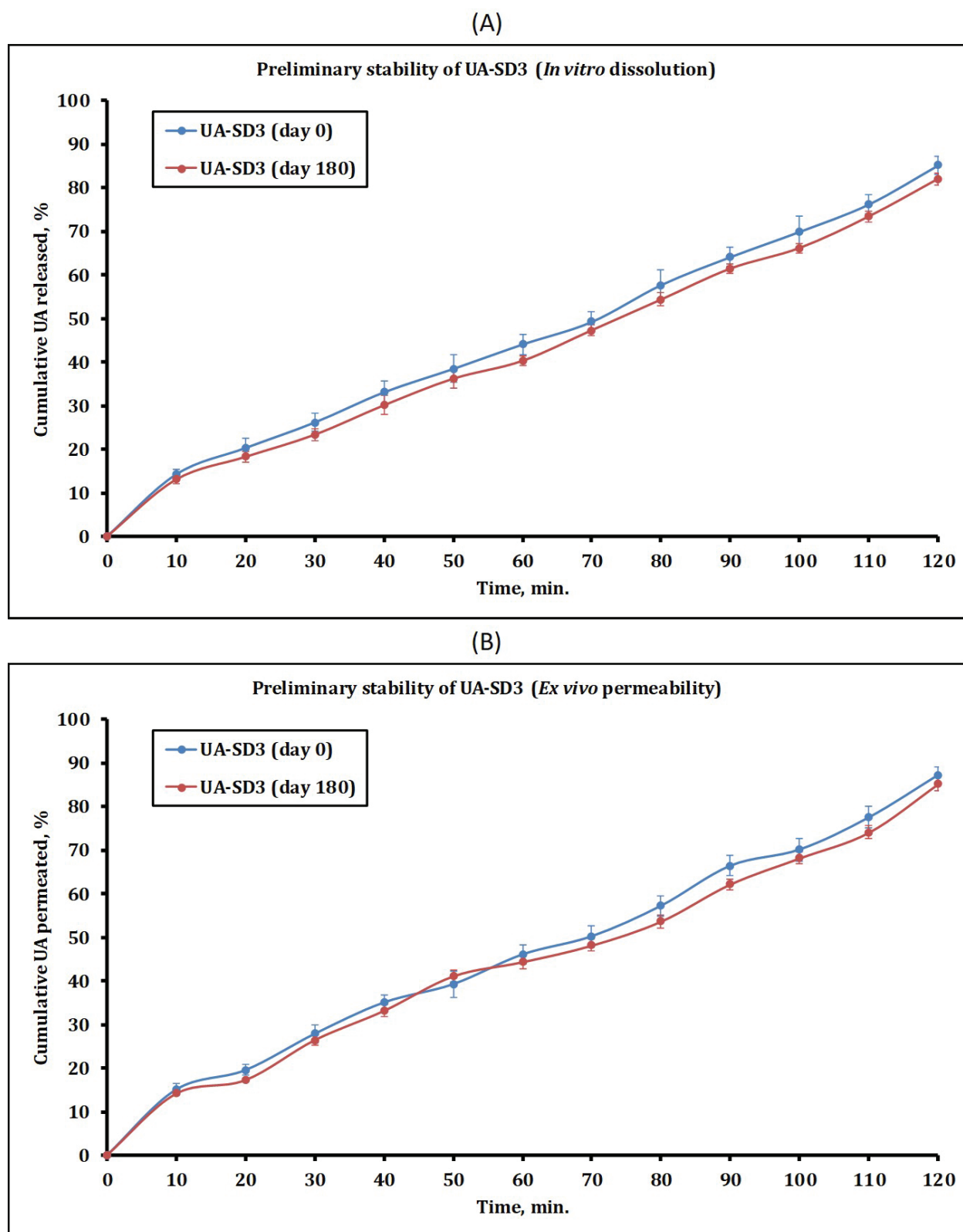


Figure 9 Preliminary stability assessment of the selected UA-SD formulation. (A) a comparison of dissolution profiles on day 0 and after six-month storage, and (B) a comparison of permeability profiles on day 0 and after six-month storage. Values are mean \pm Std. Dev. ($n = 3$).

REFERENCES

- 1 Rossi, S.S., Converse, J.L., and Hofmann, A.F., *High pressure liquid chromatographic analysis of conjugated bile acids in human bile: simultaneous resolution of sulfated and unsulfated lithocholyl amidates and the common conjugated bile acids*. J. Lipid Res., 1987. 28(5): p. 589-95
- 2 Scalia, S., *Group separation of free and conjugated bile acids by pre-packed anion-exchange cartridges*. J. Pharm. Biomed. Anal., 1990. 8(3): p. 235-41
- 3 Setchell, K.D. and Matsui, A., *Serum bile acid analysis*. Clin. Chim. Acta, 1983. 127(1): p. 1-17
- 4 Danzinger, R.G., Hofmann, A.F., Schoenfield, L.J., and Thistle, J.L., *Dissolution of Cholesterol Gallstones by Chenodeoxycholic Acid*. N. Engl. J. Med., 1972. 286(1): p. 1-8.10.1056/nejm197201062860101
- 5 Perez, M.J. and Briz, O., *Bile-acid-induced cell injury and protection*. World J. Gastroenterol., 2009. 15(14): p. 1677-89
- 6 Scholmerich, J., Becher, M.S., Schmidt, K., Schubert, R., Kremer, B., Feldhaus, S., and Gerok, W., *Influence of hydroxylation and conjugation of bile salts on their membrane-damaging properties—studies on isolated hepatocytes and lipid membrane vesicles*. Hepatology, 1984. 4(4): p. 661-6
- 7 Poupon, R.E., Balkau, B., Eschwège, E., and Poupon, R., *A Multicenter, Controlled Trial of Ursodiol for the Treatment of Primary Biliary Cirrhosis*. N. Engl. J. Med., 1991. 324(22): p. 1548-1554.10.1056/nejm199105303242204
- 8 Scalia, S., Pazzi, P., Stabellini, G., and Guarneri, M., *HPLC assay of conjugated bile acids in gastric juice during ursodeoxycholic acid (Deursil) therapy of bile reflux gastritis*. J. Pharm. Biomed. Anal., 1988. 6(6-8): p. 911-7
- 9 Earnest, D.L., Holubec, H., Wali, R.K., Jolley, C.S., Bissonette, M., Bhattacharyya, A.K., Roy, H., Khare, S., and Brasitus, T.A., *Chemoprevention of azoxymethane-induced colonic carcinogenesis by supplemental dietary ursodeoxycholic acid*. Cancer Res., 1994. 54(19): p. 5071-4
- 10 Kohno, H., Suzuki, R., Yasui, Y., Miyamoto, S., Wakabayashi, K., and Tanaka, T., *Ursodeoxycholic acid versus sulfasalazine in colitis-related colon carcinogenesis in mice*. Clin. Cancer Res., 2007. 13(8): p. 2519-25.10.1158/1078-0432.ccr-06-2727
- 11 Martinez-Moya, P., Romero-Calvo, I., Requena, P., Hernandez-Chirlaque, C., Aranda, C.J., Gonzalez, R., Zarzuelo, A., Suarez, M.D., Martinez-Augustin, O., Marin, J.J., and de Medina, F.S., *Dose-dependent antiinflammatory effect of ursodeoxycholic acid in experimental colitis*. Int. Immunopharmacol., 2013. 15(2): p. 372-80.10.1016/j.intimp.2012.11.017
- 12 Yoshikawa, M., Tsujii, T., Matsumura, K., Yamao, J., Matsumura, Y., Kubo, R., Fukui, H., and Ishizaka, S., *Immunomodulatory effects of ursodeoxycholic acid on immune responses*. Hepatology, 1992. 16(2): p. 358-64
- 13 Igimi, H. and Carey, M.C., *pH-Solubility relations of chenodeoxycholic and ursodeoxycholic acids: physical-chemical basis for dissimilar solution and membrane phenomena*. J. Lipid Res., 1980. 21(1): p. 72-90
- 14 Moroi, Y., Kitagawa, M., and Itoh, H., *Aqueous solubility and acidity constants of cholic, deoxycholic, chenodeoxycholic, and ursodeoxycholic acids*. J. Lipid Res., 1992. 33(1): p. 49-53
- 15 Li, Y., Wang, Y., Yue, P.F., Hu, P.Y., Wu, Z.F., Yang, M., and Yuan, H.L., *A novel high-pressure precipitation tandem homogenization technology for drug nanocrystals production - a case study with ursodeoxycholic acid*. Pharm. Dev. Technol., 2014. 19(6): p. 662-70.10.3109/10837450.2013.819015
- 16 Ma, Y.Q., Zhang, Z.Z., Li, G., Zhang, J., Xiao, H.Y., and Li, X.F., *Solidification drug nanosuspensions into nanocrystals by freeze-drying: a case study with ursodeoxycholic acid*. Pharm. Dev. Technol., 2016. 21(2): p. 180-8.10.3109/10837450.2014.982822
- 17 Ventura, C.A., Tirendi, S., Puglisi, G., Bousquet, E., and Panza, L., *Improvement of water solubility and dissolution rate of ursodeoxycholic acid and chenodeoxycholic acid by complexation with natural and modified β -cyclodextrins*. Int. J. Pharm., 1997. 149(1): p. 1-13. [https://doi.org/10.1016/S0378-5173\(96\)04821-1](https://doi.org/10.1016/S0378-5173(96)04821-1)
- 18 Yue, P.-F., Zhang, W.-J., Yuan, H.-L., Yang, M., Zhu, W.-F., Cai, P.-L., and Xiao, X.-H., *Process Optimization, Characterization and Pharmacokinetic Evaluation in Rats of Ursodeoxycholic Acid-Phospholipid Complex*. AAPS PharmSciTech, 2008. 9(1): p. 322-329.10.1208/s12249-008-9040-1
- 19 Damian, F., Blaton, N., Naesens, L., Balzarini, J., Kinget, R., Augustijns, P., and Van den Mooter, G., *Physicochemical characterization of solid dispersions of the antiviral agent UC-781 with polyethylene glycol 6000 and Gelucire 44/14*. Eur. J. Pharm. Sci., 2000. 10(4): p. 311-322. [https://doi.org/10.1016/S0928-0987\(00\)00084-1](https://doi.org/10.1016/S0928-0987(00)00084-1)
- 20 Leuner, C. and Dressman, J., *Improving drug solubility for oral delivery using solid dispersions*. Eur. J. Pharm. Biopharm., 2000. 50(1): p. 47-60. [https://doi.org/10.1016/S0939-6411\(00\)00076-X](https://doi.org/10.1016/S0939-6411(00)00076-X)
- 21 Serajuddin, A.T.M., *Solid dispersion of poorly water soluble drugs: Early promises, subsequent problems, and recent breakthroughs*. J. Pharm. Sci., 1999. 88(10): p. 1058-1066. <https://doi.org/10.1021/js980403l>
- 22 Chiou, W.L. and Riegelman, S., *Preparation and dissolution characteristics of several fast-release solid dispersions of griseofulvin*. J. Pharm. Sci., 1969. 58(12): p. 1505-10
- 23 Dhore, P.W., Dave, V.S., Saoji, S.D., Bobde, Y.S., Mack, C., and Raut, N.A., *Enhancement of the aqueous solubility and permeability of a poorly water soluble drug ritonavir via lyophilized milk-based solid dispersions*. Pharm. Dev. Technol., 2017. 22(1): p. 90-102.10.1080/10837450.2016.1193193
- 24 Telange, D.R., Patil, A.T., Pethe, A.M., Fegade, H., Anand, S., and Dave, V.S., *Formulation and characterization of an apigenin-*

- phospholipid phytosome (APLC) for improved solubility, in vivo bioavailability, and antioxidant potential.* Eur. J. Pharm. Sci., 2017. 108: p. 36-49. <https://doi.org/10.1016/j.ejps.2016.12.009>
- 25 Telange, D.R., Patil, A.T., Pethe, A.M., Tatode, A.A., Anand, S., and Dave, V.S., *Kaempferol-phospholipid complex: formulation, and evaluation of improved solubility, in vivo bioavailability, and antioxidant potential of kaempferol.* J. Excip. Food. Chem., 2016
- 26 Choudhary, A., Rana, A.C., Aggarwal, G., Kumar, V., and Zakir, F., *Development and characterization of an atorvastatin solid dispersion formulation using skimmed milk for improved oral bioavailability.* Acta Pharmaceutica Sinica B, 2012. 2(4): p. 421-428. <https://doi.org/10.1016/j.apsb.2012.05.002>
- 27 Al-Hamidi, H., Edwards, A.A., Mohammad, M.A., and Nokhodchi, A., *To enhance dissolution rate of poorly water-soluble drugs: glucosamine hydrochloride as a potential carrier in solid dispersion formulations.* Colloids Surf. B Biointerfaces, 2010. 76(1): p. 170-8.10.1016/j.colsurfb.2009.10.030
- 28 Klein, S., *The Use of Biorelevant Dissolution Media to Forecast the In Vivo Performance of a Drug.* The AAPS Journal, 2010. 12(3): p. 397-406.10.1208/s12248-010-9203-3
- 29 Dixit, P., Jain, D.K., and Dumbwani, J., *Standardization of an ex vivo method for determination of intestinal permeability of drugs using everted rat intestine apparatus.* J. Pharmacol. Toxicol. Methods, 2012. 65(1): p. 13-7.10.1016/j.vascn.2011.11.001
- 30 Saoji, S.D., Belgamwar, V.S., Dharashivkar, S.S., Rode, A.A., Mack, C., and Dave, V.S., *The Study of the Influence of Formulation and Process Variables on the Functional Attributes of Simvastatin-Phospholipid Complex.* Journal of Pharmaceutical Innovation, 2016. 11(3): p. 264-278.10.1007/s12247-016-9256-7
- 31 Saoji, S.D., Raut, N.A., Dhore, P.W., Borkar, C.D., Popielarczyk, M., and Dave, V.S., *Preparation and Evaluation of Phospholipid-Based Complex of Standardized Centella Extract (SCE) for the Enhanced Delivery of Phytoconstituents.* AAPS J., 2016. 18(1): p. 102-14.10.1208/s12248-015-9837-2
- 32 Petros, R.A. and DeSimone, J.M., *Strategies in the design of nanoparticles for therapeutic applications.* Nat. Rev. Drug Discovery, 2010. 9: p. 615.10.1038/nrd2591
- 33 Hou, Z., Li, Y., Huang, Y., Zhou, C., Lin, J., Wang, Y., Cui, F., Zhou, S., Jia, M., Ye, S., and Zhang, Q., *Phytosomes loaded with mitomycin C-soybean phosphatidylcholine complex developed for drug delivery.* Mol. Pharm., 2013. 10(1): p. 90-101.10.1021/mp300489p
- 34 Yonemochi, E., Ueno, Y., Ohmae, T., Oguchi, T., Nakajima, S.-i., and Yamamoto, K., *Evaluation of Amorphous Ursodeoxycholic Acid by Thermal Methods.* Pharm. Res., 1997. 14(6): p. 798-803.10.1023/a:1012114825513
- 35 Balcerowiak, W., *Comments on pentaerythritol DSC.* J. Therm. Anal. Calorim., 1996. 46(6): p. 1881-1883.10.1007/bf01980791
- 36 Ramamoorthy, P. and Krishnamurthy, N., *Vibration spectrum of pentaerythritol.* Spectrochimica Acta Part A: Molecular and Biomolecular Spectroscopy, 1997. 53(5): p. 655-663. [https://doi.org/10.1016/S1386-1425\(96\)01849-5](https://doi.org/10.1016/S1386-1425(96)01849-5)
- 37 Goldberg, A.H., Gibaldi, M., and Kanig, J.L., *Increasing Dissolution Rates and Gastrointestinal Absorption of Drugs via Solid Solutions and Eutectic mixtures III: Experimental Evaluation of Griseofulvin—succinic Acid Solid Solution.* J. Pharm. Sci., 1966. 55(5): p. 487-492. <https://doi.org/10.1002/jps.2600550508>
- 38 Goldberg, A.H., Gibaldi, M., Kanig, J.L., and Mayersohn, M., *Increasing dissolution rates and gastrointestinal absorption of drugs via solid solutions and eutectic mixtures. IV. Chloramphenicol-urea system.* J. Pharm. Sci., 1966. 55(6): p. 581-3
- 39 Konno, H., Handa, T., Alonzo, D.E., and Taylor, L.S., *Effect of polymer type on the dissolution profile of amorphous solid dispersions containing felodipine.* Eur. J. Pharm. Biopharm., 2008. 70(2): p. 493-499. <https://doi.org/10.1016/j.ejpb.2008.05.023>
- 40 Raman, S. and Polli, J.E., *Prediction of positive food effect: Bioavailability enhancement of BCS class II drugs.* Int. J. Pharm., 2016. 506(1-2): p. 110-5.10.1016/j.ijpharm.2016.04.013